Designing Real Nanotube-Based Gas Sensors

A. R. Rocha,[1,2] M. Rossi,[1,*] A. Fazzio,[1,2] and Antonio J. R. da Silva[1,†]

[1]*Instituto de Física, Universidade de São Paulo, CP 66318, 05315-970, São Paulo, SP, Brazil*
[2]*Centro de Ciências Naturais e Humanas, Universidade Federal do ABC, Santo André, SP, Brazil*

(Received 14 December 2007; published 29 April 2008)

Using a combination of density functional theory and recursive Green's functions techniques, we present a full description of a large scale sensor, accounting for disorder and different coverages. Here, we use this method to demonstrate the functionality of nitrogen-rich carbon nanotubes as ammonia sensors as an example. We show how the molecules one wishes to detect bind to the most relevant defects on the nanotube, describe how these interactions lead to changes in the electronic transport properties of each isolated defect, and demonstrate that there are significative resistance changes even in the presence of disorder, elucidating how a realistic nanosensor works.

DOI: 10.1103/PhysRevLett.100.176803 PACS numbers: 73.63.Fg, 07.07.Df, 71.23.−k, 72.10.Bg

The area of gas sensors has gained a lot of attention due to our current concern over environmental and health issues [1]. One-dimensional nanosensors such as carbon nanotubes (CNT) [2], semiconductor nanowires [3], and graphene nanoribbons [4] can remedy many of the drawbacks of traditional semiconductor-based gas sensors [1,5]. Within this class of materials, CNTs have a set of unique and outstanding properties [6] that make them ideal candidates for nanosensors. Recently, it has been experimentally observed that nanotubes can present significant resistance changes upon exposure to a variety of gases [2].

The interaction of many molecules with the walls of pristine nanotubes is, however, not very strong, and a strategy to remedy this situation is to functionalize them, possibly via exohedral or substitutional doping [7,8]. In that aspect, nitrogen as a substitutional dopant has been investigated both experimentally [9] as well as theoretically [10]. Besides single atom doping, a new family of nanotube materials, the highly nitrogen-doped carbon nanotubes (CN_x), has been recently synthesized [11]. In a recent work, these CN_x nanotubes have been assembled in films that have shown functionality as sensors to a variety of gases, such as ammonia, acetone, ethanol and chloroform [12]. It has been argued that the reason these tubes present such behavior is due to the interaction between the molecule in question and the nitrogen defects present in the nanotube. In essence, the defect would serve as a binding site for the molecule leading to changes in the electronic structure and subsequently in the transport properties of the overall system. It has also been proposed that the N atoms in CN_x nanotubes are arranged in pyridine-like "cavities"; a particular atomic configuration that has been suggested consists of three nitrogen atoms around a vacancy site—a three-nitrogen vacancy (3NV) [11]. However, we have recently shown that a four-nitrogen divacancy (4ND) has a formation energy which is lower by more than 1 eV for a wide range of chemical potentials and is, consequently, the most stable defect in CN_x nanotubes [13]. The reaction path that leads an NH_3 molecule, to bind to either nitrogen defect is yet unknown, and it is one of the aims of this work.

Atomistic simulations are a great predictive tool that can help in designing better devices. In order to perform quantitatively meaningful simulations of realistic sensors, however, one must consider the fact that these devices most often can reach the 100 nm length scale with a large number of randomly distributed defects. Therefore, the effect of disorder is an issue that must also be taken into consideration. Thus far, this aspect has hindered theoretical efforts.

In this Letter, we demonstrate how a scheme based on *ab initio* density functional theory (DFT) calculations, coupled with recursive Green's functions methods [14–16], allows: 1) an understanding of the detailed properties of individual defects, with the identification of the most relevant ones; 2) a detailed description of the interaction of the molecules to be detected with these defects; 3) the charge transport properties of the individual, isolated, defects; 4) and finally and most importantly, a full description of a large scale sensor, with disorder and different coverage taken into account. Here, we expand the formalism presented by Gómez-Navarro *et al.* [14] to use the full Hamiltonian in orbital representation coming from DFT calculations which allows for the evaluation of the electronic transport properties of realistic nanoscopic sensors with great accuracy and speed. Because of the availability of experimental data and a demonstrated ability to act as sensors, we focus on CN_x nanotubes as an example of how we can create a new paradigm in the field of sensor design, where computer simulations can treat realistic systems and, via close interaction with experimentalists, can help design more efficient and highly sensitive nanodevices.

All our calculations were performed on single-walled (5,5) carbon nanotubes with 9 irreducible cells (~ 180 atoms). We considered the two possible nitrogen defects mentioned earlier, namely, the 3NV and the 4ND, whose fully relaxed structures [17] are shown in Figs. 1(a) and 1(b) 1.

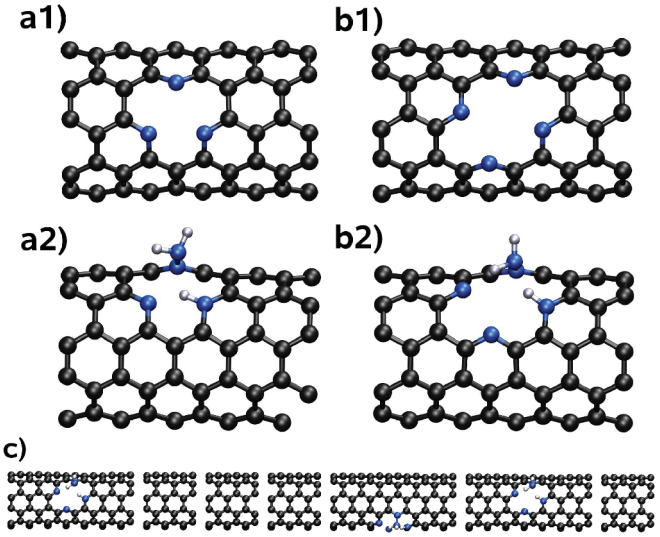

FIG. 1 (color). Different CN_x CNTs after relaxation: (a) 3NV, (b) 4ND in the cases 1) without and 2) with ammonia. For clarity the structures have been rotated around the tube axis and only the central section of the supercell is shown. c) Example of a disordered CN_x structure. Color code: carbon: black, nitrogen: blue, hydrogen: light blue.

For the transport calculations, we initially follow the procedure described by Caroli *et al.* [18]. There, the system is divided into three parts, namely, the left- and right-hand side electrodes and a central scattering region. The electrodes were taken as pristine (5,5) nanotubes whereas the scattering region consists of either a nanotube with a single defect or 180-nm-long nanotube with defects randomly distributed—both in distance and rotation angle—along the tube. The defect concentration per mass was kept at approximately 0.5%. Because of the strong coupling with the electrodes, we do not consider self-interaction corrections [19].

The central quantity for determining the transport properties of our system is the Green's function for the scattering region which is defined as

$$G = [E \times S_S - H_S - \Sigma_L - \Sigma_R]^{-1}, \qquad (1)$$

where E is the energy, H_S and S_S are the Hamiltonian and Overlap matrices for the scattering region, and Σ_L and Σ_R are the so-called self-energies, the effect of the coupling to the electrodes [15,20].

The calculation using *ab initio* methods of such a long system would render the problem intractable. Therefore, we further split the Hamiltonian of the scattering region into segments as depicted in Fig. 1(c). Each element consists of either a pristine (5,5) nanotube or one of the defect structures in Figs. 1(a) and 1(b) which can also be rotated with respect to each other. Each segment is computed in a separate SIESTA calculation and the Hamiltonian and Overlap matrices are stored. They are then used as building blocks for H_S and S_S [32]. One can then use the fact that H_S and S_S are block-tridiagonal, and that we are only interested in the terms of the Green function that couple left and right electrodes to recursively reduce the Hamiltonian of the entire device to a renormalized Hamiltonian for the electrodes with an effective coupling [15,16]. This effective Hamiltonian can then be used to calculate the total transmission, $T(E)$ using the Nonequilibrium Green's function formalism [20–22] for coherent transport in the linear regime [33]. The DOS were also calculated via Green's functions, thereby avoiding problems related to the periodicity of the DFT calculation. Finally, in the low bias limit, the conductance is given by

$$g = \frac{dI}{dV}\bigg|_{V\to 0} = \int T(E)\frac{df(E')}{dE'}\bigg|_E dE, \qquad (2)$$

where $f(E)$ is the Fermi distribution function for a given temperature T.

We start our analysis by looking at the dissociation of ammonia molecules onto these two types of defects. The NH_3 molecule was placed on top of one of the nitrogens in either the 3NV or the 4ND. The resulting fully relaxed structures are show in Figs. 1(a) and 1(b) 2. In both cases, we observed a barrierless dissociation process [23]. In other words, by bringing the NH_3 molecule close to the defect, it naturally breaks up into an NH_2 molecule and a hydrogen atom that bind to two different nitrogens on the defect. The binding energies for each case are $E_b = -0.26\ eV$ and $E_b = -0.02\ eV$ for the 3NV and 4ND, respectively. In the latter case, such a small biding energy is a strong indication that the NH_3 molecule can be easily removed by either heating up the CN_x nanotube or by an air stream [11].

We have also considered the situation whereby the NH_3 dissociates onto a pristine nanotube. Both in the case of NH_2 + H and NH + 2H complexes attached to the CNT, the process is endothermic by more than 1 eV. Consequently, in agreement with previous studies [24], it is unlikely that NH_3 will attach to the side walls of pristine CNTs. Henceforth, we assumed that the molecule only binds to the defects.

Before moving on to calculate the transport properties of realistic sensors, it is important to understand the characteristics of a single isolated defect in the cases with and without ammonia. The resulting zero-bias transmission curves and DOS are shown in Fig. 2. From the DOS, we can clearly see that both for the ammonia-free 3NV and the 4ND nanotubes, there are localized states approximately 0.5 eV bellow the Fermi level, E_F. These states can be associated with the nitrogens of the defect. After binding to the nitrogen atoms, the ammonia molecule has the property of removing those states from the energy window. Despite this similarity, the transport properties of these two systems are rather different from each other. In the 4ND case, the transmission around the Fermi level decreases as the ammonia molecule binds to the site. On the other hand, the molecule in the 3NV case, rather interestingly, has the

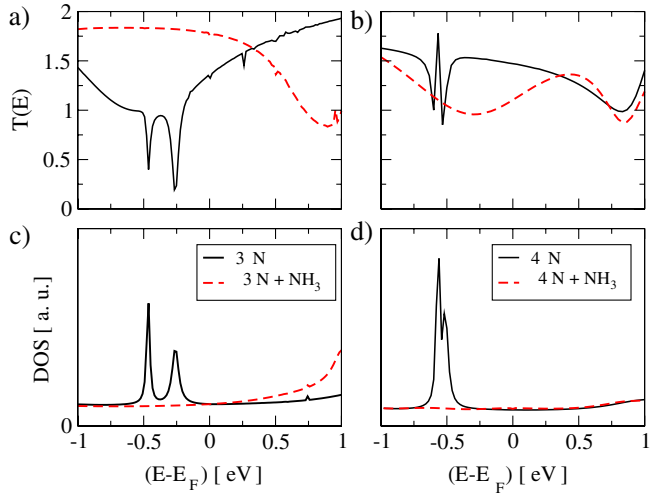

FIG. 2 (color online). Transmission coefficients (a), (b) and DOS (c), (d) for CN_x nanotubes with three- and four-nitrogen defects. The solid (dashed) line shows the results without (with) ammonia dissociated on the defect.

effect of repairing the nanotube and the total transmission approaches 2, that of a pristine CNT.

A fully functioning device, however, contains a large number of defects. It is also very likely that, upon exposure to a particular molecule, not all binding sites will react. The coverage of the tube is then an important quantity that can ultimately be used to determine the sensitivity of our device. Hence, we simulated the conductance at room temperature of long nanotube sensors considering defects with and without ammonia in different complimentary proportions. Since we have random distributions of defects, for each concentration of ammonia, we performed up to 300 realizations, and the average and standard deviation were calculated. In Fig. 3, we show the average of the low-bias conductance as a function of ammonia coverage in the 3NV case. We observe close to 1 order of magnitude decrease in conductance as the ammonia concentration decreases. This qualitatively corroborates the trend observed in the single-defect transmission curves, in other words, that the dissociation of ammonia causes an increase in conductance. On the other hand, the fact that our device now has a large number of defects leads to a distribution of values for the conductance. In the strong Anderson-localization regime [25], one would expect the distribution of the natural logarithm of the conductance to follow a Gaussian distribution with a variance associated with the type of defect as well as the concentration. In fact, we can see from the inset of Fig. 3 that this is indeed the case. A Gaussian fit to the representative quantity $\ln g$ is in good agreement with this assumption yielding a variance $\Delta = 0.23$.

The trend observed for the 4ND CN_x is quite the opposite. The results which are shown in Fig. 4 clearly point to a reduction in the conductance with increasing ammonia coverage of the divacancy site. This suggests, together with our total energy calculations [13], that the type of defect most likely to be present in these nanotubes is not the pyridine-like defect as it was previously thought [11], but most likely the four-nitrogen divacancy.

More interesting, however, is the change in the average conductance as a function of ammonia concentration. In the single-defect calculation, we observed a conductance change of approximately 40% upon ammonia dissociation, whereas a large number of randomly distributed defects leads to a factor of 5 variation. This result is extremely important for device fabrication because it indicates that the sensitivity of our device can be extremely high, and that it is a viable technological option. We can observe significant changes even at reasonably low ammonia concentrations. At the same time, the low binding energy makes the ammonia molecules easily removed, by, for example, slightly increasing the temperature of the device. This could be easily achieved by increasing the bias voltage

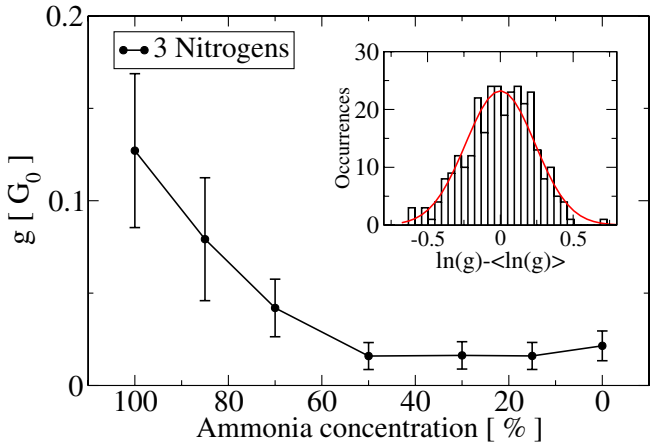

FIG. 3 (color online). Average of the conductance (in units of $G_0 = 2e^2/h$), as a function of ammonia concentration for 3NV in CN_x nanotubes. The inset shows a histogram of conductance values for the 3NV defects in the presence of ammonia.

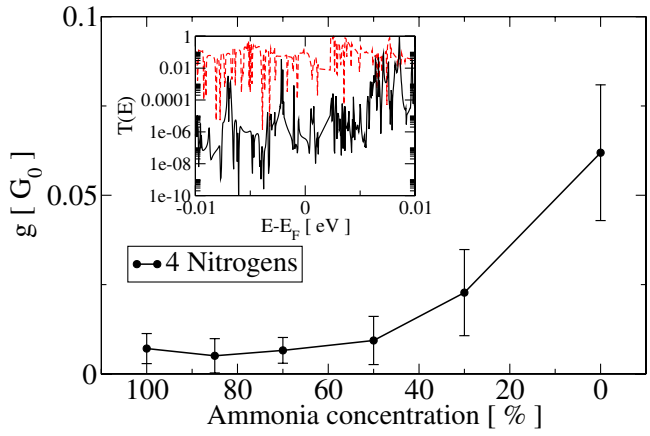

FIG. 4 (color online). Average of the conductance (in units of $G_0 = 2e^2/h$) as a function of ammonia concentration for 4ND. The inset shows typical transmission curves as a function of energy with 0 % (solid line) and 100 % (dashed line) coverage.

across the nanotube, since it has been reported that the melting temperature of CNTs is over 2500 K even in the presence of defects [26]. The result is a nanosensor that can be reutilized several times.

Hence, we have identified, with a combination of DFT and Green's function-based electronic transport methods, what is the most likely defect present in CN_x nanotubes and the mechanism behind the experimentally observed resistance changes. Importantly, we have also observed that nitrogen defects can act as catalysts for the dissociation process. Finally, it was shown how CN_x nanotubes can be used as nanosensors for ammonia molecules with high sensitivity even at very low concentrations. Although the analysis of a single defect can give some insight into the problem of electronic transport in nanosensors, only a calculation including the effects of disorder and coverage leads to quantitatively meaningful results for realistic sensors.

In conclusion, we have presented a combination of methods that can be applied to a variety of different one-dimensional systems that can act as sensors. The procedure we described has the power of becoming a paradigm in nanosensors design since it allows, via total energy calculations, the identification of the relevant defect structures and how they interact with the foreign species. Then, via *ab initio* charge transport calculations, we characterize the transmittance properties of each individual structure of interest. Finally, we designed a procedure that allows the study of realistic large scale sensors with disorder, and which permits the investigation of the sensor behavior as a function of coverage. Although there is still much work to be done, including the issue of poisoning by other species and the effects of the electrodes, our method can help determine optimal defect type and concentration for obtaining the highest sensitivity.

The authors are indebted to FAPESP for financial support (Grants Nos. 05/59581-6 and 06/57338-0). The calculations were performed using the HPC cluster at USP (FAPESP No. 05/54190-9) and UFABC.

*Present address: Fritz-Haber-Institut der Max-Planck-Gesellschaft, Faradayweg 4-6, D-14195 Berlin (Dahlem), Germany

†ajrsilva@if.usp.br

[1] N. Yamazoe, Sens. Actuators B Chem. **108**, 2 (2005).
[2] J. Kong *et al.*, Science **287**, 622 (2000).
[3] Y. Cui, Q. Wei, H. Park, and C. M. Lieber, Science **293**, 1289 (2001).
[4] F. Schedin *et al.*, Nat. Mater. **6**, 652 (2007).
[5] Y.-T. Jang *et al.*, Sens. Actuators B Chem. **99**, 118 (2004).
[6] M. S. Dresselhaus, G. Dresselhaus, and P. Avouris, eds., *Carbon Nanotubes: Synthesis, Structure, Properties and Applications*, Topics in Applied Physics Series (Springer, Heidelberg Germany, 2001).
[7] K. Jiang *et al.*, Nano Lett. **3**, 275 (2003).
[8] P. Qi *et al.*, Nano Lett. **3**, 347 (2003).
[9] Y.-M. Choi *et al.*, Nano Lett. **3**, 839 (2003).
[10] H. J. Choi, J. Ihm, S. G. Louie, and M. L. Cohen, Phys. Rev. Lett. **84**, 2917 (2000).
[11] M. Terrones *et al.*, Appl. Phys. A **74**, 355 (2002).
[12] F. Villalpando-Páez *et al.*, Chem. Phys. Lett. **386**, 137 (2004).
[13] M. A. Rossi, A. Fazzio, and A. J. R. da Silva, Phys. Rev. B (to be published).
[14] C. Gómez-Navarro *et al.*, Nat. Mater. **4**, 534 (2005).
[15] S. Sanvito, C. J. Lambert, J. H. Jefferson, and A. M. Bratkovsky, Phys. Rev. B **59**, 11936 (1999).
[16] T. Markussen, R. Rurali, M. Brandbyge, and A.-P. Jauho, Phys. Rev. B **74**, 245313 (2006).
[17] In order to avoid basis superposition errors [28], the binding energies were calculated with the plane wave code VASP [29] using a cutoff of 290 eV, ultrasoft pseudopotentials, and the PW91-GGA for the exchange-correlation potential. The reaction paths and subsequent atomic relaxations were also calculated using SIESTA [30]. Again, the relaxations were performed with GGA [31] using a DZP basis set for all the atoms, an energy shift of 0.03 eV and a real-space grid cutoff of 300 Ry. The final structures were identical in both codes.
[18] C. Caroli, R. Combescot, P. Nozieres, and D. Saint-James, J. Phys. C **5**, 21 (1972).
[19] C. Toher, A. Filippetti, K. Burke, and S. Sanvito, Phys. Rev. Lett. **95**, 146402 (2005).
[20] A. R. Rocha *et al.*, Phys. Rev. B **73**, 085414 (2006).
[21] M. Brandbyge *et al.*, Phys. Rev. B **65**, 165401 (2002).
[22] F. D. Novaes, A. J. R. da Silva, and A. Fazzio, Braz. J. Phys. **36**, 799 (2006).
[23] See EPAPS Document No. E-PRLTAO-100-055816 for movies of the Conjugate Gradient evolution of the dissociation process of ammonia molecules on the two types of defects that can be downloaded from the EPAPS website. For more information on EPAPS, see http://www.aip.org/pubservs/epaps.html.
[24] J. Andzelm, N. Govind, and A. Maiti, Chem. Phys. Lett. **421**, 58 (2006).
[25] B. Kramer and A. MacKinnon, Rep. Prog. Phys. **56**, 1469 (1993).
[26] K. Zhang, G. M. Stocks, and J. Zhong, Nanotechnology **18**, 285703 (2007).
[27] M. S. Purewal *et al.*, Phys. Rev. Lett. **98**, 186808 (2007).
[28] S. Boys and F. Bernardi, Mol. Phys. **19**, 553 (1970).
[29] G. Kresse and J. Furthmüller, Comput. Mater. Sci. **6**, 15 (1996).
[30] D. Sánchez-Portal, P. Ordejón, E. Artacho, and J. M. Soler, Int. J. Quantum Chem. **65**, 453 (1997).
[31] J. P. Perdew, K. Burke, and M. Ernzerhof, Phys. Rev. Lett. **77**, 3865 (1996).
[32] For the transport calculations, we used a double-ζ basis. Calculations using DZP were also performed with no significant changes to the results.
[33] Coherent transport in CNTs up to 500 nm long has been demonstrated even in the presence of defects [27].